Satellite Characterization: Angles and Light Curve Data Fusion for Spacecraft State and Parameter Estimation

Moriba K. Jah
Oceanit Laboratories, Inc., 590 Lipoa Parkway, Suite 259, Kihei, HI 96753
Ronald A. Madler
Embry-Riddle Aeronautical University, 3700 Willow Creek Road, Prescott, AZ 86301

ABSTRACT

One of the challenges of satellite characterization is the ability to determine the spacecraft orientation, size, and material properties. A substantial amount of research has been conducted into using photometry and spectroscopy to give insight into these spacecraft properties, but this work has been traditionally decoupled from the orbit determination process. Data fusion is an eventual tool in the spacecraft characterization community. The reality is that the spacecraft non-gravitational dynamics are influenced by the effects of solar radiation pressure, which are precisely a function of the heliocentric spacecraft position and orientation with associated material properties. By using data types that are sensitive to spacecraft position, attitude, and material properties, not only should orbit determination be possible, but this may constrain the estimates of spacecraft properties yielding more realistic results. Another benefit of the data fusion in the estimation process is that the correlations between spacecraft states and associated properties are captured within the covariance matrix. Hence, the uncertainties in these parameters are readily available. Errors in the spacecraft modeling are mapped into spacecraft state errors and vice versa. This work describes the capability of satellite characterization achieved by fusing angles and light curve data in a sigma-point filter framework called Optical Data Estimation for Space Situational Awareness (ODESSA). Since ODESSA is a current-state filter, this capability reflects what can be achieved in near-real time. A backward smoother capability was extended to ODESSA, as a means of recovering the best possible estimates based upon all of the data.

1. INTRODUCTION

Space Situational Awareness (SSA) is an attempt to make sense out of space-related data based on the comprehension of their meaning (context). Relevant questions are: what assets are in orbit? Who do they belong to? What is their purpose/intention? What can these assets do? What will they do next? What is their operational status? Satellite Characterization attempts to be a tool which provides the capability to answer these questions. Current research in this topic has proven to yield satisfactory results, however, the methods employed require large amounts of data from varied sources and extensive computational resources. This prevents the results from being available in a timely manner. Another caveat to this current research is that the uncertainties in the characterization itself are not quantified in a straightforward fashion. Kalman filtering is a method that provides both straightforward uncertainty quantification and yields near real-time parameter estimates in the presence of noisy and potentially biased data.

The Joint Directors of Laboratories (JDL) defines Data Fusion [1] as "the process dealing with the association, correlation, and combination of data and information from single and multiple sources to achieve refined position and identity estimates, and complete and timely assessments of situation and threats, and their significance. The process is characterized by continuous refinements of its estimates and assessments, and by evaluation of the need for additional sources, or modification of the process itself, to achieve improved results." Data Fusion is what enables SSA. Kalman filtering is an architecture that is suitable for Data Fusion since it can process data from multiple sensors to yield optimal state estimates and associated uncertainties.

Prior work has shown that accurate angles data can be used to accurately update orbit information in near real time [2] and that light curves can be inverted to provide attitude and shape information [3]. This work describes the capability of satellite characterization achieved by fusing angles and light curve data in a sigma-point (Unscented Kalman) filter framework called ODESSA. Since ODESSA is a current-state filter, this capability reflects what can be achieved in near-real time. A backward smoother capability was extended to ODESSA, as a means of recovering the best possible estimates based upon all of the data available.

2. METHODS AND PROCEDURES

In order to assess the usefulness of this approach for improved satellite characterization within SSA, two research routes can be taken: apply the theory to directly process the actual optical data or follow a development path that first simulates the light curve and angles data before applying the filter to the actual observation data. The benefit of first simulating the data is that one knows exactly what is in the data so that the filter tuning process can proceed in an incremental fashion. However, this method can only theoretically demonstrate the usefulness of this approach for SSA. Processing actual data is a necessary capability. The chosen research path is to simulate these data in increasingly complex scenarios until acceptable results are obtained for scenarios that are as close to reality as possible. Then, this approach can be extended to processing actual data. This incremental development approach is desired since reality is rarely ideal.

ODESSA is a set of MATLAB routines created and intended for use in the support of SSA research and development. ODESSA processes astrometric and photometric data as orbit determination measurements. It estimates and propagates the translational states of a vehicle[1]. Knowing that the trajectory reconstruction will be based on measurements that are noisy and potentially biased and using some given combination of kinematics and dynamics, the total state vector formulation is partitioned in the following way:

$$\bar{\mathrm{X}}_{\mathrm{T}} = \begin{Bmatrix} \mathrm{X}_{\mathrm{k}} \\ \hline \mathrm{X}_{\mathrm{pm}} \\ \hline \mathrm{X}_{\mathrm{pd}} \end{Bmatrix} = \begin{Bmatrix} \text{6-element state sub-vector} \\ \hline \mathrm{N}_{\mathrm{m}}\text{-element measurement model parameter sub-vector} \\ \hline \mathrm{N}_{\mathrm{d}}\text{-element dynamics model parameter sub-vector} \end{Bmatrix}$$

The ODESSA state sub-vector X_k is defined as:

$$\mathbf{X}_k = \begin{bmatrix} s/c\ position \\ s/c\ velocity \end{bmatrix} = \begin{bmatrix} x & y & z & \dot{x} & \dot{y} & \dot{z} \end{bmatrix}^T_{ECI}$$

where: s/c is spacecraft center and ECI is the Earth Centered Inertial (J2000) coordinate frame.

The ODESSA measurement model parameter sub-vector X_{pm} is comprised of the telescope location on the Earth, the one-way-light-time (OWLT)[2] from the spacecraft to the telescope, and the angles data biases respectively. It is defined as:

$$\mathbf{X}_{pm} = \begin{bmatrix} x_{site} & y_{site} & z_{site} & OWLT & \alpha_{bias} & \delta_{bias} \end{bmatrix}^T$$

The ODESSA dynamic model parameter sub-vector X_{pd} is comprised of the spacecraft material properties and size in terms of specular reflectivity, diffuse reflectivity, emissivity, and projected area respectively. It is defined as:

$$\mathbf{X}_{pd} = \begin{bmatrix} C_{spec} & C_{diff} & C_{emis} & A \end{bmatrix}^T$$

Since ODESSA employs a current-state filter, an Extended Kalman Filter (EKF) is typically used. However, the EKF has a few drawbacks, namely that it only works well with systems which are near-linear on the time scale of the measurement updates, it requires Jacobians of relationships that can be very complicated to implement, and these filters can also be notoriously cumbersome to tune[3][4]. This has motivated novel approaches in non-linear system estimation. One such novel method was introduced by Julier and Uhlmann (1997) [4] called the Unscented Kalman Filter. The term "Unscented" comes from the fact that this filter implementation makes use of the Unscented Transformation.

---

[1] ODESSA has a working version of a 6DOF filter which estimates and propagates both the translational and rotational states of the vehicle. However, this version has only been tested with inertial sensor data.

[2] Although the OWLT is part of the estimate list, stellar aberration is not being taken into account in these simulations. For actual data processing, stellar aberration will be appropriately accounted for.

[3] Tuning a filter refers to the process of selecting the appropriate measurement noise, process noise, and other parameters to which the filter output is sensitive to, that yield acceptable state estimates. At a basic level, what is tuned is the Kalman gain, to yield the optimal state estimate.

Several features of this filter are that no explicit derivatives (Jacobians) are required [5], no linearization is required, and the dynamics are propagated through their modeled non-linearities. Given an *a priori* mean and covariance for the state error, a set of points (states) is sampled. Although similar to a Monte Carlo, the difference lies in that the sampled points are not being randomly drawn based upon the *a priori* statistics but rather drawn based upon a minimum set of deterministically chosen weighted points which completely capture the true mean and covariance of the prior random variable [6]. When these points, called Sigma Points, are propagated through the modeled nonlinear system, the *a posteriori* mean and covariance are captured accurately to the 2nd order for any non-linearity[4].

A backward smoothing capability was extended to the UKF, making it a UKS (Unscented Kalman Smoother) [7]. This smoothing algorithm is analogous to the traditional Rauch-Tung-Striebel (RTS) smoother used in linearized Kalman filters. This work presents both the best current-state the best smoothed state.

The simulated light curve data were generated with an anisotropic Phong BRDF model [8]. The model is a sum of a diffuse term and a specular term. This model was used because of its analytic ease of implementation and because it has several desirable properties:

1. obeys energy conservation and reciprocity laws
2. allows anisotropic reflection
3. accounts for Fresnel behavior, where specularity increases with decreasing incidence angle
4. has a non-constant diffuse term, so the diffuse component decreases with decreasing incidence angle

The general methodology is as follows:

1. Take a set of initial conditions and spacecraft characteristics and generate an ephemeris (truth trajectory).
2. Generate observations on that truth trajectory, corrupting them with white noise and biases.
3. Perturb the true initial conditions, adding significant error (i.e. true orbit and spacecraft parameters are not known).
4. Define realistic *a priori* state uncertainties (i.e. an initial state covariance).
5. Define measurement data weights (i.e. measurement noise covariance).
6. Fit the data with the filter and assess performance based upon how well the filter is able to recover the true spacecraft trajectory and characteristics.
7. Adjust (and/or include) process noise parameters (and *a priori* state covariance if needed).
8. Repeat steps 6 and 7 until scenario results are acceptable.
9. Add incremental complexity/realism to simulation scenario, repeating step 1 through 9 until scenarios are as near to realism as possible.
10. Apply filter to fit actual data and assess performance based on how well the filter is able to recover a near true trajectory (perhaps taken from a high accuracy orbit solution of another agency) or by how well the recovered orbit and spacecraft parameters are able to predict future observations.
11. Repeat step 10 until results are acceptable.

3. RESULTS

The results shown are those achieved by processing data from one site. Multiple sites may provide added dimensionality to the data reduction and is part of future work. Light curve and angles data were simulated at a frequency of 5 seconds[5], for a nominal geosynchronous orbit based on the TDRS 5 orbit. These data were corrupted by Gaussian white noise, and biased. The true spacecraft was modeled as a 60 m^2 sun-pointed flat plate made of Multi-Layer Insulation (MLI). ODESSA was initialized with a perturbed initial state vector and the assumed spacecraft model was a 10 m^2 sun-pointed flat plate made of solar cells. The spacecraft dynamics were modeled using a 10x10 truncated gravity field (EGM96) and solar radiation pressure. Data were only generated for elevation angles above 10 degrees and Earth shadow was accounted for. The following figure shows the simulated orbit, with portions in black representing those portions of the orbit where data were generated. The simulated groundstation was located in California (Mohave Desert).

[4] For Gaussian distributions, 3rd order accuracies are expected.

[5] Although these synthetic data are simultaneously observed, this need not be the case in order to process these data in ODESSA.

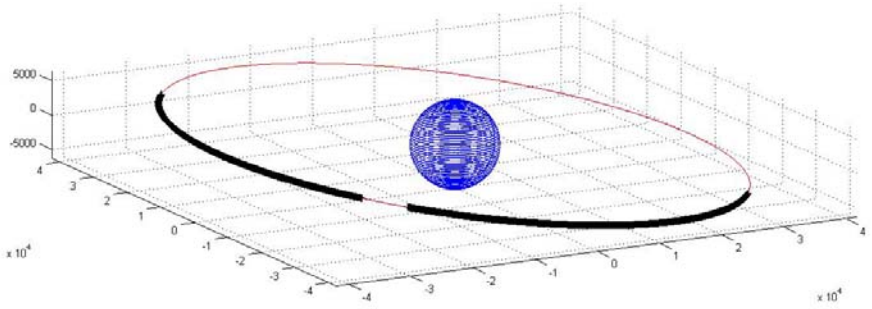

Fig. 1. Simulated geostationary orbit. Portions in black represent arcs where angles and light curve data were generated. The gap short gap between data arcs represents the portion of the trajectory within Earth shadow. All axes are in units of kilometers.

The baseline filter assumptions used for the simulated cases are shown in Table 1. They represent the 1σ *a priori* state and parameter uncertainties as well as the data weights employed.

Table 1. Baseline Filter Assumptions

Estimated Parameters	***A Priori* Uncertainty (1σ)**	**Remarks**
Position	10000 meters	1e-5 m/s^2 radial and intrack Q 1e-5 m/s^2 xtrack Q
Velocity	100 meters/sec	1e-5 m/s^2 radial and intrack Q 1e-5 m/s^2 xtrack Q
Telescope Location	100 meters	1e-20 m/s^2 process noise
RA/DEC Bias	10 arcseconds	1e-5 arcsec/sec process noise
Specular, Diffuse, Emissivity Coefficients	0.33	1e-10 sec-1 process noise
Spacecraft Area	33 m2	1e-2 m^2/sec process noise
Data Parameters	**Data Weights**	**Remarks**
Right Asc./Declination	5 arcseconds	Data noise assumed to be at 5 sec sampling rate
Brightness Magnitude	10 Mag	Data noise assumed to be at 5 sec sampling rate

The light curves that were simulated are shown in Fig. 2. The curve represents the apparent visible magnitude as a function of phase angle, where phase angle is defined as the absolute Sun-Probe-Observer (SPO) angle.

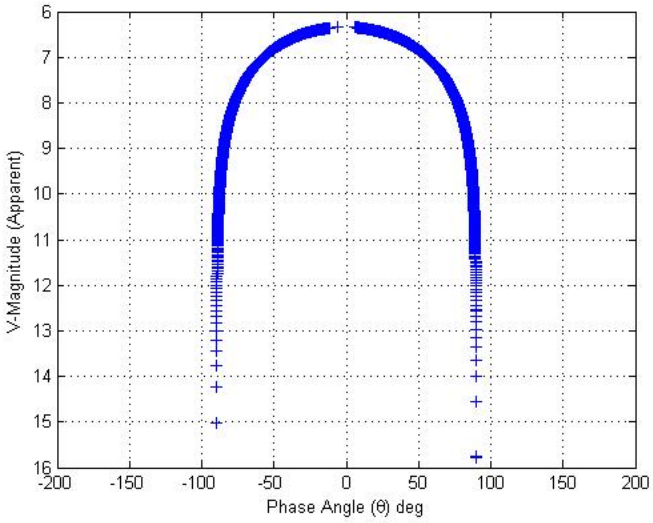

Fig. 2. Simulated light curves using an anisotropic Phong BRDF model.

In order to better assess the filter performance, spacecraft position and velocity errors and uncertainties are expressed in the Radial-Intrack-Crosstrack (R-I-C) frame. The difference between the true spacecraft position and the resultant position estimates reported by the filter and smoother, are shown in Fig. 3, in terms of the RIC frame. The results are shown in a "close-up" scale, as initial errors are off of the plot.

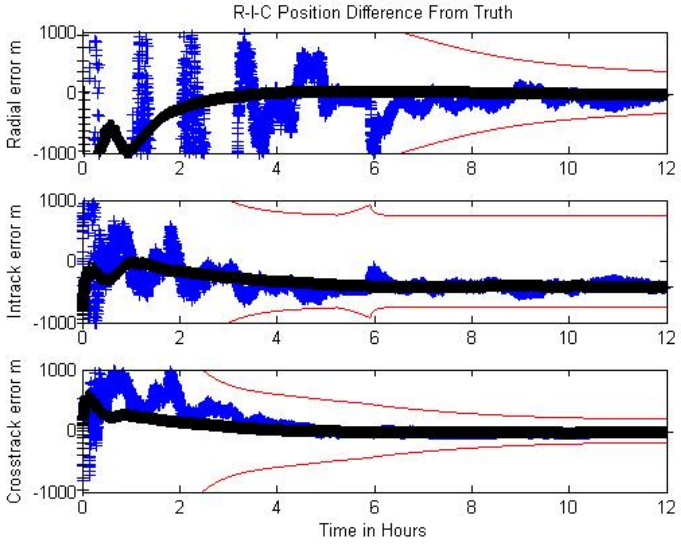

Fig. 3. Radial, Intrack, and Crosstrack filtered and smoothed position differences from the "truth" trajectory. The results from the filter (current-state) are in blue. The smoothed estimates are in black. The results are bounded by the +/- 3σ filter uncertainties in each axis, in red.

The perturbation to the initial state was on the order of 7 kilometers. The radial and crosstrack components are recovered to within 40 meters of the true trajectory. The intrack component is recovered to 400 meters. The reason for this is that the angles data were biased in Right Ascension and Declination. Because the spacecraft was observed from only one site and the spacecraft-telescope relative motion was almost purely in Declination, the filter was unable to recover an intrack error and Right Ascension bias, simultaneously. This is a problem of parameter observability in an estimation sense. In a scenario where the biases were perfectly known *a priori* (i.e. via an assumed calibration), the intrack component was also recovered to within 40 meters as shown in the total error in

Fig. 8. The simulated data biases were restricted to 2 arcseconds for each angle. The main reason for this is based upon historical data sets which seem to exhibit biases within this range. Fig. 4 is a plot showing the capability of the filter in recovering these biases.

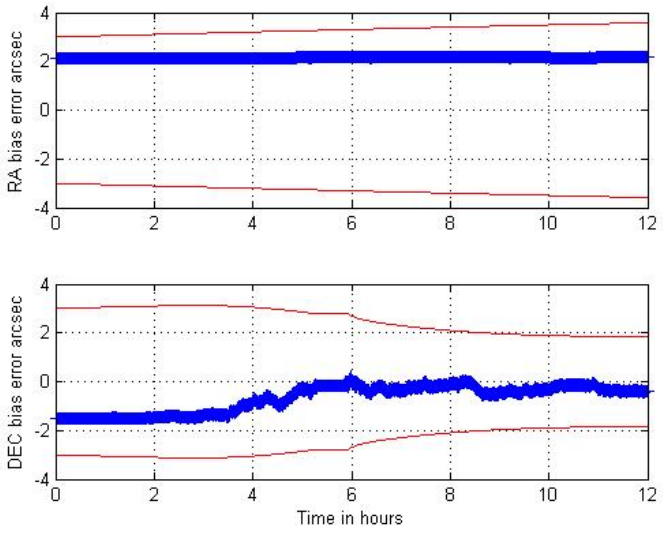

Fig. 4. Right Ascension and Declination bias estimates differenced from the true data biases, bounded by their associated +/- 3σ filter uncertainties in red.

It is clearly seen that the Right Ascension bias was unobserved by the filter for reasons previously stated. However, the filter is able to do an acceptable job in recovering the Declination bias. Another filter performance metric is the quantification of how powerful are the data in reducing state uncertainty. In order to understand the uncertainties in each axis, these are plotted against each other in Fig. 5.

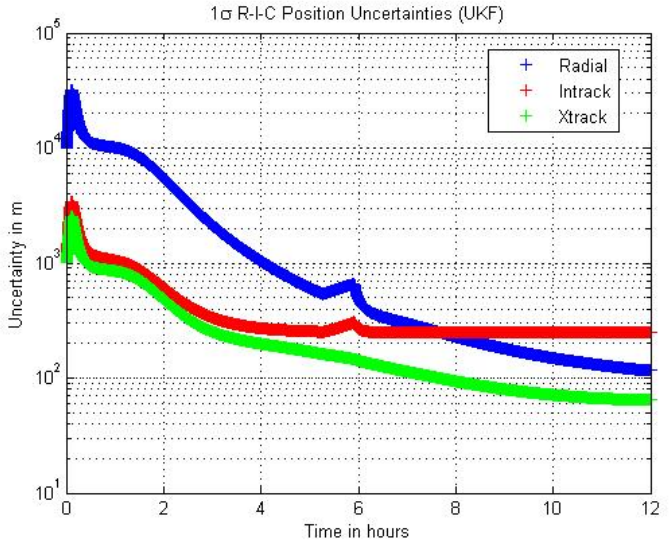

Fig. 5. Radial, Intrack, and Crosstrack 1σ position filter uncertainties

The radial component is the least determined at first. This should make sense given that the angles data are mostly plane-of-sky (perpendicular to line-of-sight) sensitive. Eventually, the radial component is well observed. The "floor" in the intrack component is in large part due to the inobservability between the bias and this component. With accurate bias calibration, this would be reduced to tens of meters versus hundreds of meters. A plot similar to Fig. 5 is shown for the RIC velocity uncertainties in Fig. 6.

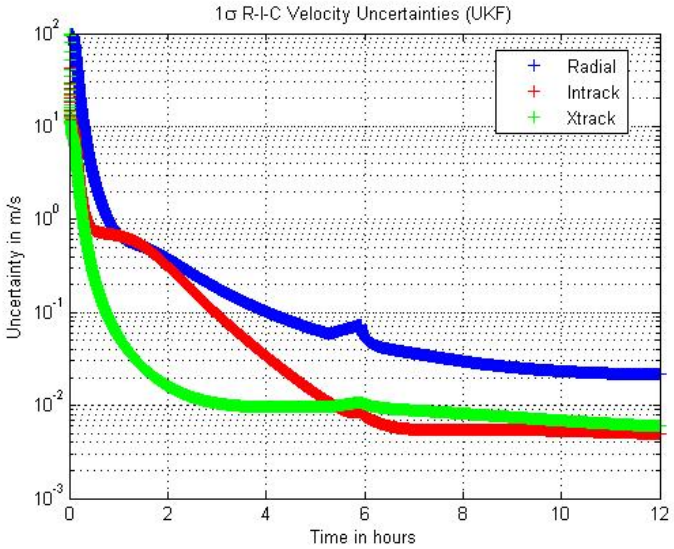

Fig. 6. Radial, Intrack, and Crosstrack 1σ velocity filter uncertainties

One interesting point to be gained from the previous figure is that if the spacecraft would have performed a thrusting maneuver with a magnitude in each axis less than the associated velocity uncertainties, it would be unlikely that this maneuver could be recovered from the data. Maneuver detection is a challenging task. Ultimately, we are interested in assessing the capability of recovering the true orbit in the presence of various error sources and noisy/biased data. The total error, being the difference between the true trajectory and the estimates reported by the filter/smoother, is shown in Fig. 7.

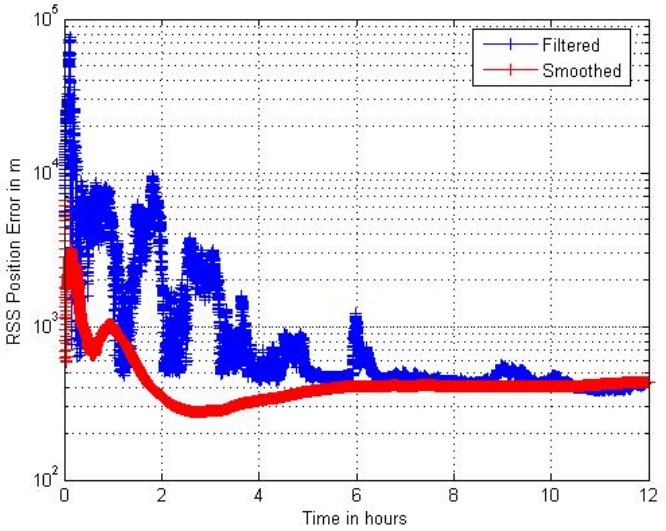

Fig. 7. RSS filter and smoother position difference from "truth". This represents the total error in position. Filter errors are in blue. Smoother errors are in red.

For this scenario, the total error is constrained to approximately 400 meters. The dominant contributor to this error in position is the error in the intrack component as was shown in Fig. 3. Again, this reduces to less than 50 meters with calibrated biases as shown in Fig. 8.

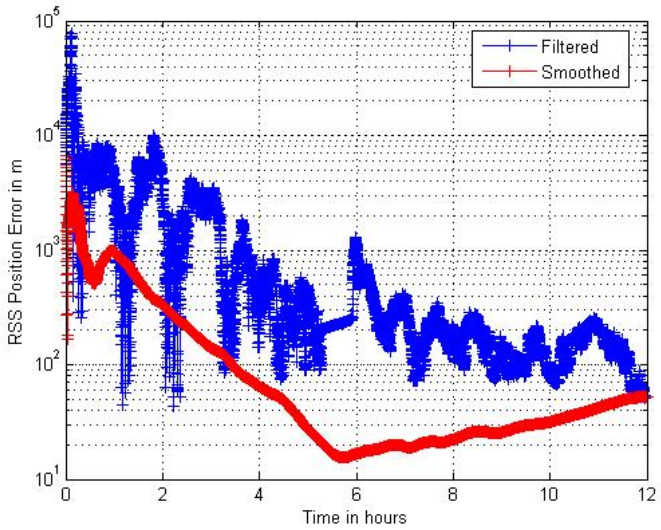

Fig. 8. RSS filter and smoother position difference from "truth". This represents the total error in position from the "perfectly known" biased data fit. Filter errors are in blue. Smoother errors are in red.

In order to gage this capability with respect to the total velocity, Fig. 9 shows the total filtered and smoothed velocity errors with respect to the truth.

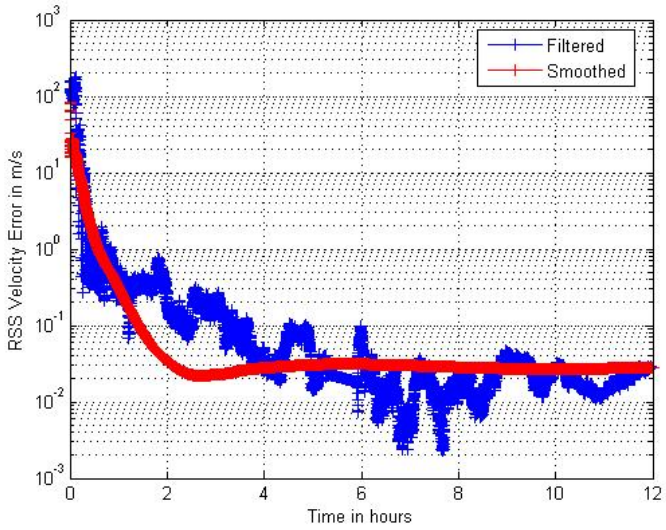

Fig. 9. RSS filter and smoother velocity difference from "truth". This represents the total error in velocity. Filter errors are in blue. Smoother errors are in red.

The total velocity error was recovered to centimeters per second. While recovering the actual orbit with quantified uncertainty is of importance for change detection, satellite characterization requires that spacecraft traits also be successfully recovered. The specular reflectivity coefficient is one of the spacecraft properties of interest and the capability in recovering the actual value is shown in Fig. 10, below.

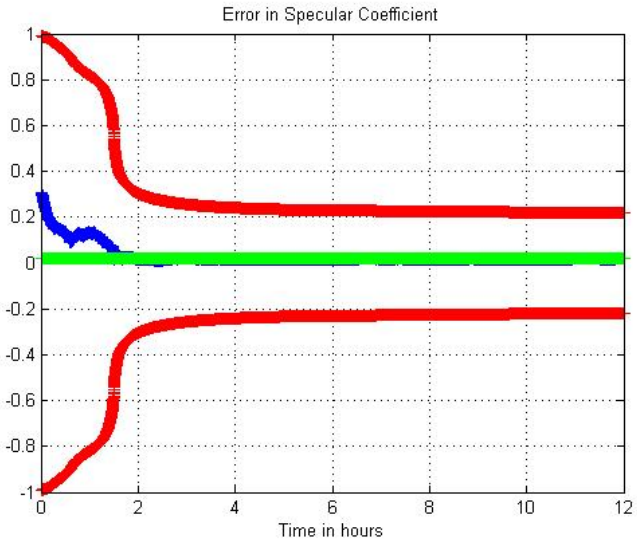

Fig. 10. Specular reflectivity coefficient filter and smoother difference from "truth" bounded by the associated +/- 3σ filter uncertainties in red. Filter errors are in blue. Smoother errors are in green.

The specular reflectivity coefficient was well observed in this scenario. In less than 2 hours, the filter is able to recover this parameter with sufficient accuracy. The fact that this parameter is well observed within 2 hours instead of 3 or 4 hours is mainly a function of relative data weighting between the angles and light curve data. Deweighting the light curve data relative to the angles tends to increase the time in which the filter is able to recover the material properties. This was verified via simulations. The smoothed results are also to within an acceptable level of error. The diffuse reflectivity and emissivity coefficients were not recovered by the filter. The *a priori* error in the diffuse coefficient was relatively small. However, it was still unrecovered. Future research will explore whether or not multi-site data improves this. The satellite characterization also includes spacecraft size. This can be associated with spacecraft projected areas. The recovery of this parameter is shown in Fig.11.

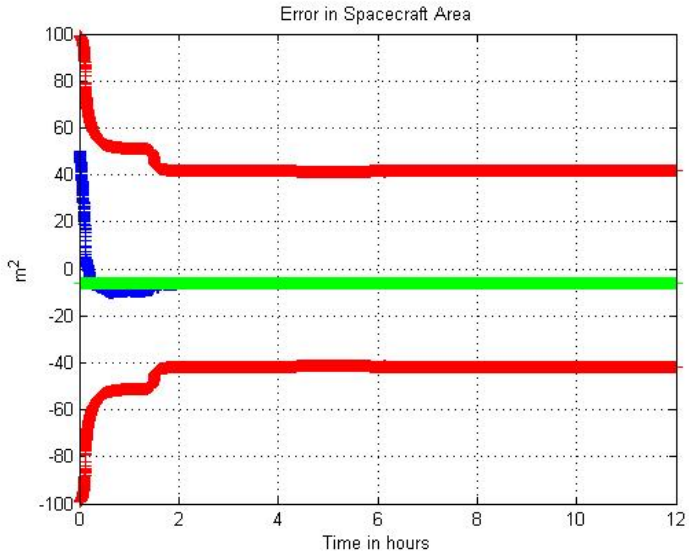

Fig. 11. Spacecraft Area filter and smoother difference from "truth" bounded by the associated +/- 3σ filter uncertainties in red. Filter errors are in blue. Smoother errors are in green.

The filter and smoother performed very well in recovering the spacecraft area. Just as with the specular coefficient, relative data weighting is the key factor driving the sensitivity for this scenario. It must be noted that none of these spacecraft traits or parameters are recovered in the absence of light curve data. Angles data alone is insufficient to provide insight into these parameters. Herein lies the power in synthesizing these two data types. They are each sensitive to different sets of parameters or states being relatively "orthogonal" to each other in an observability sense. An analysis of the partial derivatives of the data with respect to the state parameters verified this fact.

4. CONCLUSIONS AND RECOMMENDATIONS

Angles and light curve data were simulated for a single observing site. The spacecraft was modeled as a 60 m^2 sun-pointed flat plate made of MLI, in a TDRS5 (geosynchronous) orbit. All of the initial conditions given to ODESSA were significantly perturbed from their true values in an effort to gage filter performance in recovering the truth in the presence of significant state errors and biased and corrupted data. Although the simulation is still not as realistic as possible, the errors incorporated give acceptable insight into the research approach employed. ODESSA was successful in recovering the true orbit to within an acceptable error, and the spacecraft was partially characterized in terms of its size and reflectance properties. These results are very encouraging, given that this case is a single-site case. Added dimensionality provided by multiple sites will be investigated. Near real time satellite characterization seems to be a possibility. Successful Space Situational Awareness depends on the capability to synthesize data sources with associated uncertainty in near real time, a capability demonstrated by ODESSA.

5. ACKNOWLEDGEMENTS

This work was performed under AFRL HANDS contract FA9451-04-C-0381. The authors would like to give thanks to Dr. Chris Sabol, AFRL, for his support toward this research endeavor.

6. REFERENCES

1. White, F.E., "A Model for Data Fusion", Proc. 1st National Symposium on Sensor Fusion, 1988.
2. Kelecy, T. and C. Sabol, "Rapid Orbit Characterization and Real-time State Vector Handoff Using High Accuracy Metrics," AMOS Technical Conference 2005 Proceedings, Maui, HI, Sept. 5-9, 2005.
3. Hall, D., J. Africano, P. Kervin, and B. Birge, "Non-imaging Attitude and Shape Determination," AMOS Technical Conference 2005 Proceedings, Maui, HI, Sept. 5-9, 2005.
4. Julier, S.J. and J.K. Uhlmann, "A New Extension of the Kalman Filter to Nonlinear Systems," in Proc. of AeroSense: The 11th Int. Symp. on Aerospace/Defense Sensing, Simulation and Controls, 1997.
5. van der Merwe, R. and E.A. Wan, "The Square-Root Unscented Kalman Filter for State and parameter-Estimation," in ICASSP-2001, Salt Lake City, Utah, May 2001.
6. van der Merwe, R., E. A. Wan & S. Julier, "Sigma-Point Kalman Filters for Nonlinear Estimation and Sensor-Fusion: Applications to Integrated Navigation", In Proceedings of the AIAA Guidance, Navigation & Control Conference (GNC), Providence, Rhode Island, August 2004.
7. Psiaki, M.L. and M. Wada, "Derivation and Simulation Testing of a Sigma-Points Smoother," *Journal of Guidance, Control, and Dynamics*, Vol. 30, No. 1, Jan.-Feb. 2007, pp. 78-86.
8. Ashikhmin, M. and P. Shirley, "An Anisotropic Phong BRDF Model," *Journal of Graphical Tools*, Vol. 5, No. 2, 2000, pp. 25-32.